PRECISION MEASUREMENTS WITH KAONS AT CERN*

Chris Parkinson

on behalf of the NA48/2 and NA62 collaborations

University of Birmingham, Edgbaston, Birmingham, United Kingdom
chris.parkinson@cern.ch

Received 30 September 2022, accepted 23 January 2023, published online 15 February 2023

The NA62 experiment at CERN took data in 2016–2018 with the main goal of measuring the $K^+ \to \pi^+\nu\bar{\nu}$ decay. The high-intensity fixed-target setup and the detector performance make the NA62 experiment particularly suited to make precision measurements of charged kaon decays. Preliminary results of the $K^\pm \to \pi^0\pi^0\mu^\pm\nu(K^{00}_{\mu 4})$ decay first observation and analysis based on NA48/2 data collected in 2003–2004 are presented. Results from studies of $K^+ \to \pi^0 e^+\nu\gamma(K^0_{e3})$ decays are reported, based on a data sample of more than 10^5 K^0_{e3} candidates recorded in 2017–2018. Preliminary results with the most precise measurements of the K^0_{e3} branching ratios and of T-asymmetry in the K^0_{e3} decay are presented. The flavour-changing neutral current decay $K^+ \to \pi^+\mu^+\mu^-$ is induced at the one-loop level in the Standard Model. Preliminary results from an analysis of the $K^+ \to \pi^+\mu^+\mu^-$ decay are reported, using a large sample of about 3×10^{12} kaon decays into two muons recorded with a downscaled dimuon trigger operating along with the main trigger. The most precise determination of the $K^+ \to \pi^+\mu^+\mu^-$ form-factor parameters a_+ and b_+ has been made by NA62 using data collected in 2017 and 2018.

DOI:10.5506/APhysPolBSupp.16.3-A10

1. Introduction

There is a well-established history of kaon physics in the CERN North Area, including the first measurement of ϵ'/ϵ and the discovery of direct charge-parity violation (CPV). The kaon physics programme at CERN is a series of fixed-target experiments observing kaon decays in flight. A proton beam at $400\,\mathrm{GeV}/c$ is extracted from the SPS in spills of $3\,\mathrm{s}$ effective

* Presented at the XIV International Conference on *Beauty, Charm and Hyperon Hadrons*, Kraków, Poland, 5–10 June, 2022.

spill length. The protons are directed onto a beryllium target, producing a secondary hadron beam that consists of about 6% kaons.

The NA48/2 experiment operated during 2003 and 2004. The experimental setup is sketched in Fig. 1 and is described in detail in [1]. The experiment had simultaneous K^+ and K^- beams selected to have a mean momentum $P_K \approx 60\,\mathrm{GeV}/c$, with $\Delta P_K/P_K \approx 3.8\%$. The beams passed through a kaon beam spectrometer (KABES) that measured the beam particle momentum with $\approx 1\%$ momentum resolution, and a time resolution of $\approx 600\,\mathrm{ps}$. Decays of $K^\pm$ inside a fiducial volume are recorded. The momenta of the charged $K^\pm$ decay products are measured with a magnetic spectrometer equipped with 4 drift chambers, two either side of a dipole magnet, located inside a vessel filled with helium. The spectrometer was followed by a scintillator hodoscope (na48-CHOD), a liquid-krypton (LKr) calorimeter, a hadronic calorimeter, and a muon veto system.

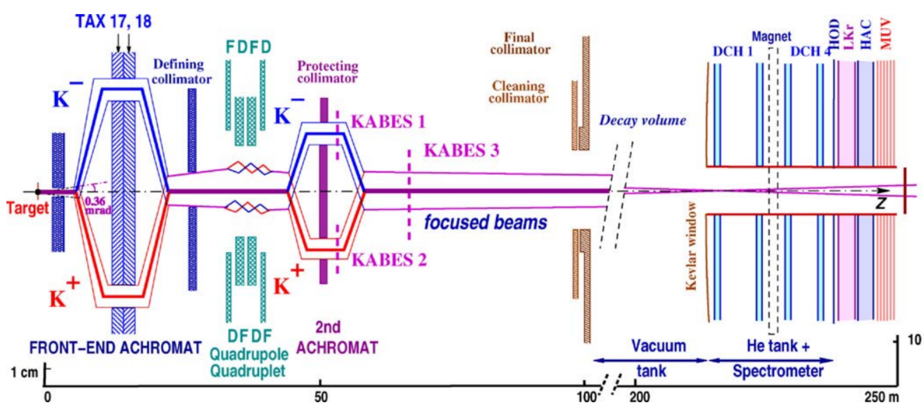

Fig. 1. Schematic side-view of the NA48/2 beam-line and detector.

The NA62 experiment has been operating since 2016 and is dedicated to measuring the $K^+ \to \pi^+\nu\bar{\nu}$ branching fraction. The experimental setup is sketched in Fig. 2 and is described in detail in [2]. The experiment has a K^+ beam only, which is selected to have a mean momentum of $P_K \approx 75\,\mathrm{GeV}/c$ and $\Delta P_K/P_K \approx 1\%$. The beam particle rate is 750 MHz. The time of each K^+ in the beam is measured with a precision of 70 ps by a differential Cherenkov counter (CEDAR) combined with a kaon tagger (KTAG). The momentum of each beam particle is measured by the GigaTracker (GTK) beam spectrometer. About 15% of the K^+ decay inside the NA62 fiducial volume. The momenta of the charged decay products are measured with a 4-chamber straw detector (STRAW), with two chambers either side of a dipole magnet, located inside a vacuum vessel. The spectrometer is followed by a Ring Imaging Cherenkov (RICH) detector, two scintillator hodoscopes

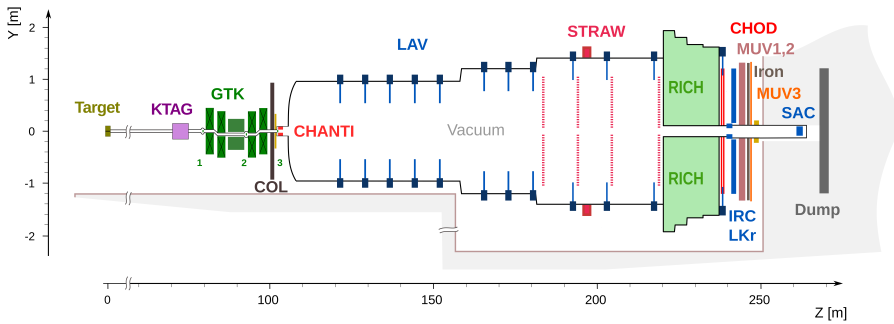

Fig. 2. Schematic side-view of the NA62 beam-line and detector.

(NA48-CHOD and CHOD), a liquid-krypton (LKr) calorimeter, an upgraded hadronic calorimeter, and an upgraded muon veto system.

2. First measurement of the $K^{\pm} \to \pi^0\pi^0\mu^{\pm}\nu$ decay

Four-body semi-leptonic kaon decays $K \to \pi\pi\ell\nu$ are described by 5 kinematic variables: S_π, the dipion invariant mass squared; S_ℓ, the dilepton invariant mass squared; θ_π (θ_ℓ), the angle between the π^+ (ℓ^+) in the dipion (dilepton) rest frame and the dipion (dilepton) system in the kaon rest frame; and ϕ, the azimuthal angle between the two planes defined by the dipion and dilepton systems in the kaon rest frame. The decay amplitude depends on form factors labelled F, G, R, and H. For the $K^{\pm} \to \pi^0\pi^0\mu^{\pm}\nu$ decay, the s-wave state has no dependence on $\cos(\theta_\pi)$ and ϕ, so only F and R contribute to the amplitude. The form of F(S_π, S_ℓ) has been determined from measurements of the $K^+ \to \pi^0\pi^0 e^+\nu$ decay [3]. A prediction for R(S_π, S_ℓ) has been computed in the context of Chiral Perturbation Theory (ChPT) [4]. The $K^{\pm} \to \pi^0\pi^0\mu^{\pm}\nu$ decay has never been observed, and there is no experimental measurement of R(S_π, S_ℓ).

The $K^{\pm} \to \pi^0\pi^0\mu^{\pm}\nu$ branching fraction is measured at NA48/2, and is normalised to the $K^{\pm} \to \pi^{\pm}\pi^0\pi^0$ decay. The two decays are selected using common criteria: 4 isolated photons consistent with $2\pi^0$ signature, matched in space and time with a KABES beam track; and a track in the drift chambers with an associated response in the muon veto system. The main background is $K^{\pm} \to \pi^{\pm}\pi^0\pi^0$ decays with the $\pi^{\pm} \to \mu^{\pm}\nu$ decay-in-flight upstream of the LKr. To mitigate this background, selection cuts are set on: the $\pi^{\pm}\pi^0\pi^0$ invariant mass and transverse momentum; the missing mass squared (M^2_{miss}), computed using the momentum of the KABES track and the combined momentum of the three pions; and $\cos(\theta_\ell)$. The remaining background contamination is measured from a fit to the data. The analysis resulted in 2437 candidates, including $354 \pm 33_{\text{stat}}$ background events.

The branching fraction is measured in a restricted phase space where $S_\ell > 0.03\,\mathrm{GeV}^2/c^4$, and the measured value is

$$\mathrm{BF}\left(K^\pm \to \pi^0\pi^0\mu^\pm\nu; S_\ell > 0.03\,\mathrm{GeV}^2/c^4\right) = (3.45 \pm 0.17) \times 10^{-6}\,.$$

This value is compatible with the theoretical prediction that includes a non-zero contribution from $\mathrm{R}(S_\pi, S_\ell)$. The branching fraction in the full phase space must be extrapolated based on theory inputs. The experimental measurement is compared to the theoretical prediction in Fig. 3.

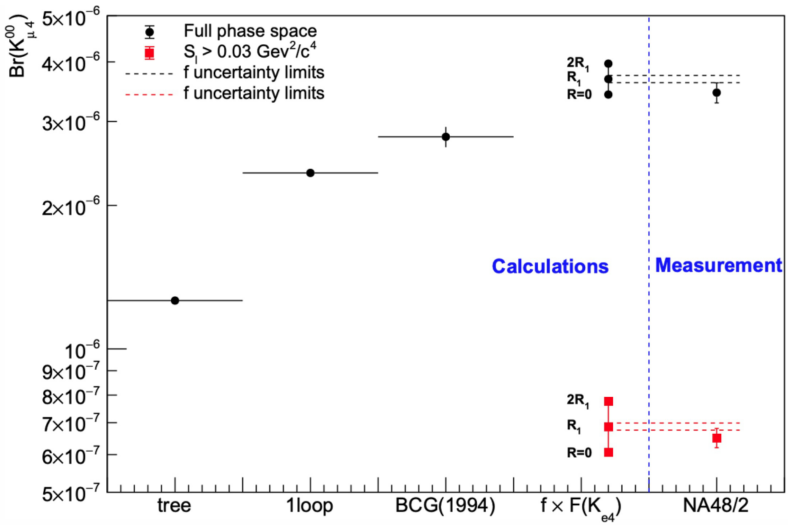

Fig. 3. Comparison of NA48/2 measurement of the $K^\pm \to \pi^0\pi^0\mu^\pm\nu$ branching fraction with theoretical predictions.

3. New study of the $K^+ \to \pi^0 e^+\nu\gamma$ decay

The $K^+ \to \pi^0 e^+\nu\gamma$ decay is a radiative kaon decay that can be described in ChPT. The final-state photon is produced either via direct emission (DE) or inner bremsstrahlung (IB), with the total amplitude including the interference between DE and IB. The IB term diverges as $E_\gamma \to 0$ and $\theta_{e,\gamma} \to 0$, where E_γ is the photon energy in the kaon rest frame and $\theta_{e,\gamma}$ is the angle between the electron and photon in the kaon rest frame. To avoid the divergences, the branching fraction is measured in three kinematic regions labelled R_j with $j = 1, 2, 3$. Table 1 gives the definition of R_j, predicted values in ChPT from [5], and the most precise measurement from [6].

Table 1. R_j definitions in terms of E_γ and $\theta_{e,\gamma}$, ChPT predictions from [5], and results of the measurements performed by the ISTRA+ [6] experiment.

	E_γ^j	$\theta_{e,\gamma}^j$	$O(p^6)$ ChPT	ISTRA+
$R_1 \times 10^2$	$E_\gamma > 10$ MeV	$\theta_{e,\gamma} > 10°$	1.804 ± 0.021	$1.81 \pm 0.03 \pm 0.07$
$R_2 \times 10^2$	$E_\gamma > 30$ MeV	$\theta_{e,\gamma} > 20°$	0.640 ± 0.008	$0.63 \pm 0.02 \pm 0.03$
$R_3 \times 10^2$	$E_\gamma > 10$ MeV	$0.6 < \cos\theta_{e,\gamma} < 0.9$	0.559 ± 0.006	$0.47 \pm 0.02 \pm 0.03$

The decay is sensitive to the T-odd observable ξ, accessible via the asymmetry A_ξ, which are defined as

$$\xi = \frac{\vec{p}_\gamma \cdot (\vec{p}_e \times \vec{p}_\pi)}{M_K^3}\,; \qquad A_\xi = \frac{N_+ - N_-}{N_+ + N_-}\,,$$

where N_+ (N_-) is the number of events with the positive (negative) value of ξ. The predictions are $|A_\xi| < 10^{-4}$ in the Standard Model (SM) and beyond [7–10], while the only measurement is $A_\xi(R_3) = 0.015 \pm 0.021$ [6].

The values of R_j and A_ξ were measured at NA62 using data collected in 2017 and 2018, with the $K^+ \to \pi^0 e^+ \nu\gamma$ measurement normalised to the $K^+ \to \pi^0 e^+ \nu$ decay. The event selection was based on associating a K^+ candidate in the KTAG and GTK with an e^+ track reconstructed in the STRAW and a $\pi^0 \to \gamma\gamma$ decay reconstructed in the LKr. The radiative photon was required to be coincident with the event and isolated from other energy deposits in the LKr. Events with other activity were rejected to suppress backgrounds from $K^+ \to \pi^0\pi^0 e^+\nu$, while additional cuts were applied to reject γ from bremsstrahlung and suppress $K^+ \to \pi^+\pi^0\pi^0$ and $K^+ \to \pi^+\pi^0$ decays. After the selection, there are about 1.3×10^5 candidates in the R_1 signal region. The measured R_j and A_ξ values are:

$$\begin{aligned}
R_1 &= (1.684 \pm 0.005 \pm 0.010) \times 10^{-2}\,, \quad & A_\xi(R_1) &= -0.1 \pm 0.3_{\rm stat} \pm 0.2_{\rm MC}\,,\\
R_2 &= (0.599 \pm 0.003 \pm 0.005) \times 10^{-2}\,, \quad & A_\xi(R_1) &= -0.3 \pm 0.4_{\rm stat} \pm 0.3_{\rm MC}\,,\\
R_3 &= (0.523 \pm 0.003 \pm 0.003) \times 10^{-2}\,, \quad & A_\xi(R_1) &= -0.9 \pm 0.5_{\rm stat} \pm 0.4_{\rm MC}\,.
\end{aligned}$$

These are the most precise measurements of R_j and $A_\xi(R_3)$, and the first measurements of $A_\xi(R_1)$ and $A_\xi(R_2)$.

4. Measurement of the $K^+ \to \pi^+\mu^+\mu^-$ decay

The $K^+ \to \pi^+\mu^+\mu^-$ decay is a flavour-changing neutral current process with a branching fraction of $O(10^{-7})$ in the SM. Although the decay is dominated by long-distance effects, short-distance physics can be extracted from the form-factor parameters a_+ and b_+. The SM predicts a_+ and b_+ to be identical in $K^+ \to \pi^+\mu^+\mu^-$ and $K^+ \to \pi^+e^+e^-$ decays, and any difference is indicative of Lepton Flavour Universality (LFU) violation. Moreover, a_+ can be related to the B anomalies in models with minimal-flavour violation [11]. The largest uncertainties on a_+ are in the muon mode.

The $K^+ \to \pi^+\mu^+\mu^-$ decay is measured at the NA62 experiment using data collected in 2017 and 2018, with the measurement normalised to the $K^+ \to \pi^+\pi^+\pi^-$ decay. Candidate events are selected by reconstructing three-track vertices, and requiring associated K^+ and dimuon signatures in the detector. Dedicated kinematic cuts are applied to suppress the dominant $K^+ \to \pi^+\pi^+\pi^-$ background. The analysis yielded 2.8×10^4 $K^+ \to \pi^+\mu^+\mu^-$ candidates.

The values of $(a_+,\ b_+)$ are extracted from the data using a fit to the z spectrum of the candidates, where $z = M^2_{\mu\mu}/M^2_K$, $M^2_{\mu\mu}$ is the dimuon invariant mass squared, and M^2_K is the K^+ invariant mass squared. The fit proceeds by reweighting the $(a_+,\ b_+)$ values of simulated events until the best description of the data is achieved, evaluated as the smallest χ^2. The fit yielded the values $a_+ = -0.592 \pm 0.015$, $b_+ = -0.699 \pm 0.058$, and the branching fraction $\mathrm{BF}(K^+ \to \pi^+\mu^+\mu^-) = (9.27 \pm 0.11) \times 10^{-8}$. The results are consistent with earlier measurements of a_+ in the muon mode and in the electron mode. There is no discrepancy with SM predictions, and no indication of LFU violation.

REFERENCES

[1] J.R. Batley *et al.*, *Eur. Phys. J. C* **52**, 875 (2007).

[2] E. Cortina Gil *et al.*, *J. Instrum.* **12**, P05025 (2017).

[3] NA48/2 Collaboration (J.R. Batley *et al.*), *J. High Energy Phys.* **2014**, 159 (2014).

[4] J. Bijnens, G. Colangelo, J. Gasser, *Nucl. Phys. B* **427**, 427 (1994).

[5] B. Kubis, E.H. Müller, J. Gasser, M. Schmid, *Eur. Phys. J. C* **50**, 557 (2007).

[6] S.A. Akimenko *et al.*, *Phys. Atom. Nucl.* **70**, 702 (2007).

[7] V.V. Braguta, A.A. Likhoded, A.E. Chalov, *Phys. Rev. D* **65**, 054038 (2002).

[8] I.B. Khriplovich, A.S. Rudenko, *Phys. Atom. Nucl.* **74**, 1214 (2011).

[9] V.V. Braguta, A.A. Likhoded, A.E. Chalov, *Phys. Rev. D* **68**, 094008 (2003).

[10] E.H. Müller, B. Kubis, U.-G. Meißner, *Eur. Phys. J. C* **48**, 427 (2006).

[11] A. Crivellin, G. D'Ambrosio, M. Hoferichter, L.C. Tunstall, *Phys. Rev. D* **93**, 074038 (2016).